22. Differences in the carbon isotopic composition of substances are expressed as $\delta^{13}C$ values, which give the per mil deviation in the $^{13}C/^{12}C$ ratio of a sample relative to that of the Pee Dee belemnite (PDB) carbonate standard:

$$\delta^{13}C = \left[\frac{(^{13}C/^{12}C)_{sample}}{(^{13}C/^{12}C)_{std}} - 1\right] \times 1000$$

23. J. Quade, T. E. Cerling, J. R. Bowman, *Nature* **342**, 163 (1989).
24. T. E. Cerling and R. L. Hay, *Quat. Res.* **25**, 63 (1986).
25. T. E. Cerling, J. Quade, S. H. Ambrose, N. E. Sikes, *J. Hum. Evol.* **21**, 295 (1991).
26. E. F. Kelly, R. G. Amundson, B. D. Marino, M. J. DeNiro, *Soil Sci. Soc. Am. J.* **55**, 1651 (1991).
27. F. I. Woodward, *Trends Ecol. Evol.* **5**, 308 (1990).
28. J. R. Ehleringer, *ibid.* **6**, 95 (1991).
29. B. N. Smith, G. E. Martin, T. W. Boutton, in *Stable Isotopes: Proceedings of the Third International Conference*, E. R. Klein and P. D. Klein, Eds. (Academic Press, New York, 1979), pp. 231–237.
30 M. Pseisker, *Plant Cell Environ.* **9**, 627 (1986).
31. We used a physiognomic vegetation classification [D. J. Pratt, P. J. Greenway, M. D. Gwynne, *J. Appl. Ecol.* **3**, 369 (1966)]. In general, woodland refers to a stand of trees with canopy cover >20%, possibly with some shrubs interspersed and a ground cover dominated by grasses and herbs. Bushland is an assemblage of shrubs with a canopy height of <6 m and canopy cover of >20%. Land dominated by grasses and herbs with a canopy cover that does not exceed 2% is classified as grassland. An increase in the proportion of C4 grasses can, in general, be interpreted as representing a decrease in canopy cover. Whereas a C4 carbon isotopic signal suggests arid adapted grasses, a C3 value does not differentiate between trees, shrubs, and montane or tropical forest grasses. To increase the resolving power of isotopic analyses of pedogenic carbonate and associated organic matter for the classification of vegetation types, we need to develop a much more comprehensive suite of isotopic profiles of modern plant communities that incorporates a lateral component, in addition to characterizing additional soil components [E. F Kelly, C. Yonker, B. D. Marino, *Am. Geophys. Union Monogr. 78* (1993), p. 233].
32. In general, modern soil carbonates and coexisting organic residue with more negative $\delta^{13}C$ values (−9 to −5 per mil), indicating a greater C3 component, were associated with more densely bushed or woodland habitats proximate to drainages. Detailed correlation of proportions of C3 and C4 plants with the isotopic signature of modern soil components is complicated by the extremely seasonal nature of many of the C4 grasses and by potential disturbance of the vegetation by domestic grazing over the last 30 years.
33. T. E. Cerling, *Palaeogeogr. Palaeoclimatol. Palaeoecol.* **97**, 241 (1992).
34. D. A. Hodell, K. M. Elmstrom, J. P. Kennett, *Nature* **320**, 411 (1986).
35. N. J. Shackleton *et al.*, *ibid.* **307**, 620 (1984).
36. T. E. Cerling, Y. Wang, J. Quade, *ibid.* **361**, 344 (1993).
37. T. E. Cerling, J. Quade, Y. Wang, J. R. Bowman, *ibid.* **341**, 138 (1989).
38. A key aspect of this study involves differentiating pedogenic carbonate from detrital or groundwater origin carbonates. The theoretical model linking vegetation to pedogenic carbonate (*17*) assumes carbonate formation in the unsaturated zone where the isotope species distribution is determined by gaseous diffusion. The original parent material of paleosols in the Tugen Hills was largely noncalcareous, and features such as leached zones were not consistently evident. The lack of parent carbonate in the sequence, however, suggests that potential contamination by nonpedogenic carbonate is minimal. Carbonate nodules were sampled at depths >40 cm to minimize potential mixing of isotopically heavy atmospheric CO_2 with biologically respired CO_2 in soil systems.
39. M.Magaritz, A. Kaufman, D. H. Yaalon, *Geoderma* **25**, 157 (1981).
40. Models relating the $\delta^{13}C$ values of bulk organic matter in paleosols to those in paleovegetation generally assume that organic residues in sediments retain the isotopic signature of original plant material. However, preferential preservation of lignoproteins and lipids, which can have $\delta^{13}C$ values 2 to 6 per mil less than the whole plant [R. Benner, M. L. Fogel, E. K. Sprague, R. E. Hodson, *Nature* **329**, 708 (1987)], as well as decarboxylation reactions during diagenesis [P. Deines, in *The Terrestrial Environment*, vol. 1 of *Handbook of Environmental Isotopic Geochemistry*, P. Fritz and J. C. Fontes, Eds. (Elsevier, New York, 1980), pp. 329–406] can lead to ^{13}C depletion in residual matter. Alternatively, preferential loss of ^{12}C during microbial oxidation can result in residual carbon enrichment by a few per mil relative to plant biomass [K. J. Nadelhoffer and B. Fry, *Soil Sci. Soc. Am. J.* **52**, 1633 (1988)]. Under these conditions, the $\delta^{13}C$ difference between soil carbonate and associated organic matter would deviate from model predictions.
41. B. F. Jacobs and C. H. S. Kabuye, *J. Hum. Evol.* **16**, 147 (1987).
42. M. E. Morgan, J. D. Kingston, B. D. Marino, *Nature* **367**, 162 (1994).
43. D. I. Axelrod and P. H. Raven, in *Biogeography and Ecology of Southern Africa*, M J. A. Werger, Ed (Junk, The Hague, Netherlands, 1978), pp. 77–130.
44. E. M. van Zinderen Bakker and J. H. Mercer, *Palaeogeogr. Palaeoclimatol. Palaeoecol.* **56**, 217 (1986).
45. G. J. Retallack, *Miocene Paleosols and Ape Habitats of Pakistan and Kenya* (Oxford Univ. Press, New York, 1991), pp. 152 and 252–256, and references therein.
46. A. Deino, L. Tauxe, M. Monoghan, R Drake, *J. Geol.* **98**, 567 (1990).
47. B. Marino and M. B. McElroy, *Nature* **349**, 127 (1991).
48. We thank K. Cheboi, B. Kamoya, P. Kiptalam, and T. Cerling for assistance in the Tugen Hills, and the government of the Republic of Kenya for research permission. Thanks also to D Pilbeam, M. Morgan, and B. Brown for comments. This work was supported by grants from the National Science Foundation (NSF), the LSB Leakey Foundation, Boise Fund, the Geological Society of America, Bill Bishop Memorial Fund, Harvard University Anthropology Department, and Sigma Xi. Additional support was provided by the Baringo Paleontological Research Project funded by NSF (A.H.) and by the U.S. Department of Energy through the National Institute of Global Environmental Change (B.D.M.)

30 December 1993; accepted 31 March 1994

Retention and 5′ Cap Trimethylation of U3 snRNA in the Nucleus

Michael P. Terns and James E. Dahlberg*

It is shown here that maturation of the m^7G-capped precursors of U3 small nuclear RNA (snRNA) occurs by a previously unknown pathway. In contrast to the 5′ m^7G-capped precursors of other snRNAs, this RNA is not exported to the cytoplasm but is retained in the nuclei of *Xenopus laevis* oocytes, where it undergoes trimethylation of its 5′ cap. The m^7G caps of most snRNA precursors are trimethylated only after transport of the RNAs to the cytoplasm. The nuclear retention and maturation of this nucleolar RNA raises the possibility that other m^7G-capped RNAs are also retained and modified in the nucleus.

The m^7G caps at the 5′ ends of RNAs made by RNA polymerase II (RNA Pol II) facilitate the efficient export of many of these transcripts from the nucleus to the cytoplasm (*1*, *2*). Precursors of the spliceosomal U1, U2, U4, and U5 small nuclear RNAs (pre-snRNAs), which are made by RNA Pol II, are convenient substrates for the study of nucleocytoplasmic RNA trafficking, because maturation of these RNAs occurs only after they have been exported to the cytoplasm. Trimethylation of their m^7G caps to $m^{2,2,7}G$ caps and transport of the RNAs back to the nucleus require the binding of Sm proteins to a sequence element common to these RNAs (*3*, *4*). Curiously, U3 RNA, a nucleolar snRNA that functions in ribosomal RNA processing, has a $m^{2,2,7}G$ cap although the RNA lacks an Sm protein binding site (*5*). Here, we show that in spite of its m^7G cap, newly made pre-U3 RNA remains in the nucleus where trimethylation of the cap occurs. Thus, the nucleolar U3 RNA is processed by a pathway distinct from that of nucleoplasmic snRNAs. This raises the possibility that other m^7G-capped precursors of nucleolar snRNAs also are retained and processed in the nucleus; this result also confirms our previous observation (*1*) that m^7G caps are not sufficient to direct RNA Pol II transcripts out of the nucleus.

To determine the nucleocytoplasmic distribution of newly made U3 RNA, we injected a X. *laevis* U3 gene into nuclei of X. *laevis* oocytes and isolated the resulting RNA from manually dissected (6) cytoplasmic and nuclear fractions (Fig. 1A). No U3 RNA was detected in the cytoplasm, although large amounts of this RNA were present in the nucleus. As expected, a precursor of U1 RNA was present in the cytoplasm, whereas the spliceosomal U6 RNA, which is made by RNA Pol III (*4*) and has a γ-mpppG cap (*7*), was not; this

Department of Biomolecular Chemistry, 1300 University Avenue, University of Wisconsin, Madison, WI 53706, USA.

*To whom correspondence should be addressed

latter RNA served as the control for the quality of oocyte fractionation. In spite of the apparent lack of a cytoplasmic phase, most of the U3 RNA was precipitable with antibodies specific for $m^{2,2,7}G$ caps but not for m^7G caps (Fig. 1B). The specificities of the antibodies for $m^{2,2,7}G$ caps and m^7G caps were confirmed by chromatographic (*8*) and electrophoretic (Fig. 1B) analyses of the precipitable RNAs.

Injection of m^7G-capped pre-U3 RNA (made in vitro) directly into nuclei allowed us to study the kinetics of trimethylation of the 5′ ends (Fig. 2, A and B). Throughout the course of this incubation, no pre-U3 RNA was detectable in the cytoplasm but almost all of the pre-U3 RNA was converted to the $m^{2,2,7}G$-capped form. To exclude the possibility that pre-U3 RNA might pass through a very small, dynamic pool in the cytoplasm, we used monoclonal antibody mAb 414, directed against glycoproteins of the nuclear pore complex (*9*), to inhibit RNA export (*10*). This antibody did not reduce the amount of $m^{2,2,7}G$ caps on newly made U3 RNA, but it completely inhibited the export and trimethylation of pre-U1 RNA (Fig. 2C). Thus, it is likely that pre-U3 RNA remained in the nucleus, where it was modified.

To test directly if m^7G-capped pre-U3 RNA could be trimethylated without participation of the cytoplasm, we injected the RNA into isolated nuclei devoid of cytoplasm and analyzed the extent of modification by precipitation with antibodies, as above. Almost half of the pre-U3 RNA was converted to the trimethylated form in these nuclei (Fig. 3). None of the m^7G-capped pre-U1 RNA that was co-injected became trimethylated, which confirms that the nuclei were free of substantial cytoplasmic contamination. We conclude that the nuclei contain a methylating activity that specifically and efficiently converts the m^7G caps of pre-U3 RNAs to $m^{2,2,7}G$ caps. We propose that U3 RNA remains in the nucleus where its 5′ cap undergoes trimethylation, in contrast to other snRNAs made by RNA Pol II, whose caps become trimethylated in the cytoplasm (*3*, *7*).

Export of pre-U3 RNA to the cytoplasm has been reported for *X. laevis* oocytes injected with rat U3 genes (*11*). We also detected some pre-U3 RNA in the cytoplasm, but only if the amounts of injected genes were ~10-fold greater than that used in Fig. 1 (*8*). The appearance of pre-U3 RNA in the cytoplasm may reflect saturation of a nuclear retention mechanism for U3 RNA under these conditions. Normally, however, a mechanism to bring U3 small nuclear ribonucleoproteins into the nucleus would be needed only after mitosis.

Trimethylation of U3 RNA can occur outside the nucleus, as it has been observed

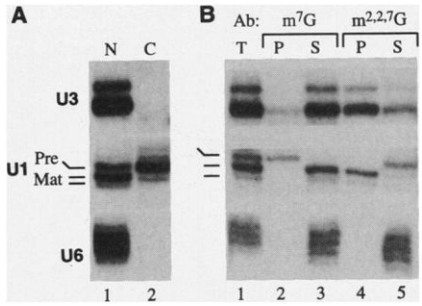

Fig. 1. Pre-U3 RNA undergoes trimethylation without appearing in the cytoplasm. (**A**) Retention of newly made pre-U3 RNA in the nucleus. U3, U1, and U6 RNAs were synthesized in *Xenopus* oocytes that had been injected in their nuclei with genes for *Xenopus* U3, U1, and U6 snRNAs (0.1, 1.0, and 0.1 ng of DNA, respectively, in 12 nl of H_2O also containing 1 μCi of [^{32}P]guanosine triphosphate) (*22*). After 6.5 hours, the ^{32}P-labeled RNAs present in one oocyte equivalent of the nuclear (N; lane 1) and cytoplasmic (C; lane 2) fractions were analyzed by polyacrylamide gel electrophoresis (*22*). The distributions of U1 and U6 RNA serve as controls for nuclear export and the quality of the oocyte dissections into nuclear and cytoplasmic fractions (*1*); the positions of precursor (pre) (m^7G-capped) and mature (mat) ($m^{2,2,7}G$-capped) U1 RNAs (*23*) are indicated. The slower migration of one form of U3 RNA presumably results from a longer 3′ end. (**B**) Trimethylation of the 5′ cap of pre-U3 RNA. The 5′ cap structures of newly synthesized snRNAs were analyzed by precipitation with antibodies specific for m^7G caps (*24*) or $m^{2,2,7}G$ caps (*25*). Nuclear RNAs (0.5 oocyte equivalents) shown in lane 1 of (A) were used for immunoprecipitation with m^7G (lanes 2 and 3) or $m^{2,2,7}G$ (lanes 4 and 5) antibodies (Ab). The RNAs present in the total sample (T, lane 1), precipitate (P, lanes 2 and 4), and supernatant (S, lanes 3 and 5) fractions were separated by polyacrylamide gel electrophoresis.

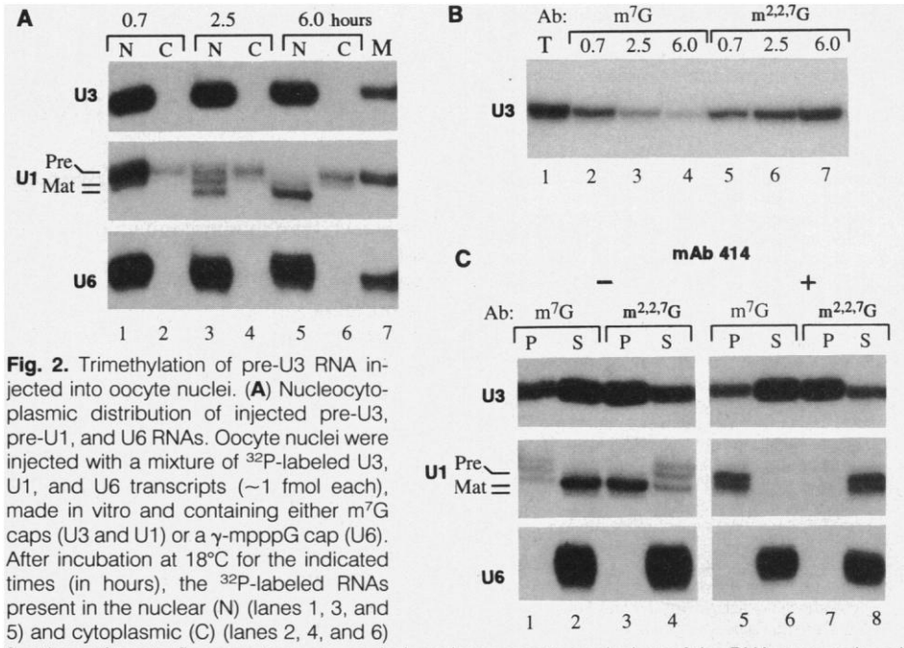

Fig. 2. Trimethylation of pre-U3 RNA injected into oocyte nuclei. (**A**) Nucleocytoplasmic distribution of injected pre-U3, pre-U1, and U6 RNAs. Oocyte nuclei were injected with a mixture of ^{32}P-labeled U3, U1, and U6 transcripts (~1 fmol each), made in vitro and containing either m^7G caps (U3 and U1) or a γ-mpppG cap (U6). After incubation at 18°C for the indicated times (in hours), the ^{32}P-labeled RNAs present in the nuclear (N) (lanes 1, 3, and 5) and cytoplasmic (C) (lanes 2, 4, and 6) fractions of two to five oocytes were pooled, and one oocyte equivalent of the RNA was analyzed by gel electrophoresis. Lane 7 (M) shows the RNAs before injection; precursor and mature forms of U1 RNA are indicated as in Fig. 1. Templates used for in vitro transcription of U1 and U6 snRNAs (with use of SP6 or T7 RNA polymerase, respectively) were as described (*1*, *22*). The U3 DNA template was similarly made by polymerase chain reaction amplification of the RNA coding sequence of the *X. laevis* U3A gene (*26*) with the use of appropriate 5′ and 3′ primer pairs. In this case, the 5′ primer contained SP6 phage RNA polymerase promoter sequences, and the resultant U3 RNA had an extra G nucleotide at its 5′ end but was otherwise identical in sequence to mature *Xenopus* U3 RNA (*27*). U3 RNA containing either one or five extra encoded nucleotides at the 3′ end behaved in a manner similar to that of U3 RNA of mature length. (**B**) Kinetics of trimethylation of injected pre-U3 RNA. U3 RNAs present in the nuclear fractions shown in lanes 1, 3, and 5 of (A) were analyzed by immunoprecipitation as in Fig. 1B. Lane 1 contains the total (T) U3 RNA present in 0.5 nuclear equivalents, and lanes 2 to 7 show the U3 RNAs that were precipitable by the antibodies at the times indicated (in hours). (**C**) Trimethylation of pre-U3 RNA occurs even when export to the cytoplasm is blocked. Oocytes were injected with ^{32}P-labeled U3, U1, and U6 RNAs synthesized in vitro in the presence (lanes 5 to 8) or absence (lanes 1 to 4) of 150 ng of a monoclonal antibody (mAb 414) against nuclear pore complex proteins (*9*). After 6.0 hours, the oocytes were dissected into nuclear and cytoplasmic fractions. The 5′ caps of RNAs present in the nuclear fraction were analyzed by immunoprecipitation as in Fig. 1B, and RNAs from both the precipitate (P; lanes 1, 3, 5, and 7) and supernatant (S; lanes 2, 4, 6, and 8) fractions were analyzed by polyacrylamide gel electrophoresis.

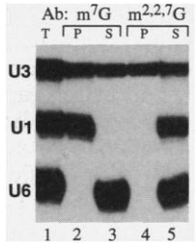

Fig. 3. Trimethylation (5′ cap) of pre-U3 RNA occurs in isolated nuclei free of the cytoplasm. A mixture of m^7G-capped U3 and U1 RNAs and γ-mpppG-capped U6 RNA (made in vitro as in Fig. 2) was injected into oocyte nuclei that had been isolated under mineral oil (*6*). After incubation at 18°C for 6.5 hours, the 5′ caps of the RNAs were analyzed as in Fig. 1B. The RNAs present in the total sample (T, lane 1) and the precipitate (P, lanes 2 and 4) and supernatant (S, lanes 3 and 5) fractions were separated by polyacrylamide gel electrophoresis.

in enucleated X. *laevis* oocytes (*11*). However, we find that trimethylation of U3 RNA in the cytoplasm is much slower than it is in the nucleus; this is in contrast with trimethylation of pre-U1 RNA, which is efficiently trimethylated in the cytoplasm (Fig. 2) (*8*). Because proteins that normally function in oocyte nuclei (but are synthesized and perhaps stored in the cytoplasm) may adventitiously modify U3 RNA in the cytoplasm, the physiological significance of cytoplasmic trimethylation of U3 RNA is unclear.

Differences in 5′ cap modification between U3 RNA and other snRNAs have also been detected in other experiments with hamster (tsBN2) tissue-culture cells. In that case, loss of RCC1 protein resulted in the inhibition of export of several snRNAs from the nucleus. This treatment inhibited trimethylation of pre-U1 and pre-U2 snRNAs but not pre-U3 RNA (*12*). These results indicate that trimethylation of pre-U3 RNA also occurs in the nuclei of mammalian somatic cells.

Although several nucleolar snRNAs have $m^{2,2,7}$G caps (*13*), others do not. For example, some of these RNAs arise from the processing of intronic sequences in pre-mRNAs, (*5, 14*) and have 5′ monophosphate termini (*15*). Moreover, in plants, where pre-U3 RNA is made by RNA Pol III (*16*), the 5′ end is modified by the addition of a methyl group to make a γ-mpppG cap (*17*). This is the same 5′ modification that occurs to U6 RNA (*18*), an RNA that also does not exit the nucleus (*1, 19*).

The discovery that U3 RNA remains in the nucleus where it undergoes trimethylation raises the question of why some precursors of snRNAs are exported from the nucleus and others are not. Generally, RNAs undergo maturation in cell compartments that are distinct from those in which they function. For example, spliceosomal snRNAs, which function in the nucleoplasm, are matured in the cytoplasm. By analogy, U3 RNA, which functions in the nucleolus (*20*), is likely to be matured in the nucleoplasm. So far, the location and identity of proteins (*21*) responsible for the stability, cap trimethylation, or nucleolar localization of U3 RNA are unknown. Several nucleolar snRNAs made by RNA Pol II, such as U3, U8, and U13 RNAs (*13*), have common sequences that are good candidates for modification signals and nucleolar localization signals. We propose that, like U3 RNA, these other $m^{2,2,7}$G-capped nucleolar snRNAs undergo maturation solely within the nucleus.

REFERENCES AND NOTES

1. M. P. Terns, J. E. Dahlberg, E. Lund, *Genes Dev.* **7**, 1898 (1993).
2. J. Hamm and I. W. Mattaj, *Cell* **63**, 109 (1990).
3. R. Lührmann, B. Kastner, M. Bach, *Biochim. Biophys. Acta* **1087**, 265 (1990); E. Izaurralde and I. W. Mattaj, *Semin. Cell Biol.* **3**, 279 (1992).
4. J. E. Dahlberg and E. Lund, in *Structure and Function of the Major and Minor Small Nuclear Ribonucleoprotein Particles*, M. L. Birnsteil, Ed. (Springer-Verlag, Heidelberg, 1988), pp. 38–70.
5. W. Filipowicz and T. Kiss, *Mol. Biol. Rep.* **18**, 149 (1993); M. J. Fournier and E. S. Maxwell, *Trends Biochem. Sci.* **18**, 131 (1993).
6. E. Lund and J. E. Dahlberg, *EMBO J.* **8**, 287 (1989).
7. R. Reddy and R. Singh, *Prog. Mol. Subcell. Biol.* **12**, 1 (1992).
8. M. P. Terns and J. E. Dahlberg, data not shown.
9. L. I. Davis and G. Blobel, *Cell* **45**, 699 (1986).
10. E. Lund, personal communication.
11. S. J. Baserga, M. Gilmore-Hebert, X. W. Yang, *Genes Dev.* **6**, 1120 (1992).
12. Y. Cheng, J. E. Dahlberg, E. Lund, unpublished results.
13. K. Tyc and J. A. Steitz, *EMBO J.* **8**, 3113 (1989); B. A. Peculis and J. A. Steitz, *Cell* **73**, 1233 (1993).
14. B. Sollner-Webb, *Cell* **75**, 403 (1993).
15. K. T. Tycowski, M. D. Shu, J. A. Steitz, *Genes Dev.* **7**, 1176 (1993).
16. T. Kiss, C. Marshallsay, W. Filipowicz, *Cell* **65**, 517 (1991).
17. S. Shimba, B. Buckley, R. Reddy, T. Kiss, W. Filipowicz, *J. Biol. Chem.* **267**, 13772 (1992).
18. R. Singh, S. Gupta, R. Reddy, *Mol. Cell. Biol.* **10**, 939 (1990).
19. J. Hamm and I. W. Mattaj, *EMBO J.* **8**, 4179 (1989).
20. R. Savino and S. A. Gerbi, *ibid.* **9**, 2299 (1990); S. Kass, K. Tyc, J. A. Steitz, B. Sollner-Webb, *Cell* **60**, 897 (1990); J. M. Hughes and M. Ares Jr., *EMBO J.* **10**, 4231 (1991).
21. K. A. Parker and J. A. Steitz, *Mol. Cell. Biol.* **7**, 2899 (1987); M. Caizergues-Ferrer, C. Mathieu, P. Mariottini, F. Amalric, F. Amaldi, *Mol. Biol. Rep.* **14**, 107 (1990); B. Lubben, C. Marshallsay, N. Rottmann, R. Lührmann, *Nucleic Acids Res.* **21**, 5377 (1993).
22. M. P. Terns, E. Lund, J. E. Dahlberg, *Mol. Cell. Biol.* **12**, 3032 (1992).
23. H. Neuman de Vegvar and J. E. Dahlberg, *ibid.* **10**, 3365 (1990).
24. T. W. Munns, M. K. Liszewski, J. T. Tellam, H. F. Sims, R. E. Rhoads, *Biochemistry* **21**, 2922 (1982).
25. P. Bringmann, J. Rinke, B. Appel, R. Reuter, R. Lührmann, *EMBO J.* **2**, 1129 (1983).
26. R. Savino, Y. Hitti, S. A. Gerbi, *Nucleic Acids Res.* **20**, 5435 (1992).
27. C. Jeppesen, B. Stebbins-Boaz, S. A. Gerbi, *ibid.* **16**, 2127 (1988).

28. We are indebted to E. Lund for suggesting the use of mAb 414 to inhibit export as well as for valuable discussions, technical advice, and comments on the manuscript. We thank also Y. Cheng, C. Grimm, V. Lyamichev, and R. Terns for useful discussions; S. Gerbi and A. Krol for kindly providing the *Xenopus* U3 and U6 genes; R. Reddy for furnishing the γ-mpppG cap analog; T. Munns and R. Lührmann for the m^7G and $m^{2,2,7}$G cap polyclonal antibodies; and D. Goldfarb for the concentrated nuclear pore protein antibodies (mAb 414). Supported by NIH grant GM30220 (J.E.D.) and NIH postdoctoral fellowship GM14704 (M.P.T.).

18 March 1994; accepted 22 April 1994

Role of Bone Marrow–Derived Cells in Presenting MHC Class I–Restricted Tumor Antigens

Alex Y. C. Huang, Paul Golumbek, Mojgan Ahmadzadeh, Elizabeth Jaffee, Drew Pardoll,* Hyam Levitsky*

Many tumors express tumor-specific antigens capable of being presented to $CD8^+$ T cells by major histocompatibility complex (MHC) class I molecules. Antigen presentation models predict that the tumor cell itself should present these antigens to T cells. However, when conditions for the priming of tumor-specific responses were examined in mice, no detectable presentation of MHC class I–restricted tumor antigens by the tumor itself was found. Rather, tumor antigens were exclusively presented by host bone marrow–derived cells. Thus, MHC class I–restricted antigens are efficiently transferred in vivo to bone marrow–derived antigen-presenting cells, which suggests that human leukocyte antigen matching may be less critical in the application of tumor vaccines than previously thought.

Despite the presence of tumor antigens capable of being recognized by T cells (*1*), the persistent growth of tumors in their host indicates that T cells specific for their antigens have not been appropriately activated in vivo (*2*). Dissection of the immune response induced by vaccination with either irradiated or genetically modified tumor cells has shown that, as with other antigens, both $CD4^+$ and $CD8^+$ T cells are involved in generating the systemic antitumor response (*3, 4*). Most likely, efficient

Department of Oncology, Johns Hopkins University School of Medicine, Baltimore, MD 21205, USA.

*To whom correspondence should be addressed.